Available online at www.sciencedirect.com
SCIENCE DIRECT®
Journal of Molecular Catalysis A: Chemical 235 (2005) 161–172
JOURNAL OF MOLECULAR CATALYSIS A: CHEMICAL
www.elsevier.com/locate/molcata

Hydrogenation catalysts formation in the system $AlEt_3$-$Co(acac)_{2,3}$

F.K. Shmidt [a], L.O. Nindakova [b,*], B.A. Shainyan [b], V.V. Saraev [a], N.N. Chipanina [b], V.A. Umanetz [a]

[a] *Department of Chemistry, Irkutsk State University, 1 Karl Marx Street, 664003 Irkutsk, Russia*
[b] *A.E. Favorsky Irkutsk Institute of Chemistry, Siberian Division of the Russian Academy of Sciences, 1 Favorsky Street, 664033 Irkutsk, Russia*

Received 19 November 2004; received in revised form 16 February 2005; accepted 18 February 2005
Available online 17 May 2005

Abstract

Formation of catalytically active species in the system $AlEt_3$-$Co(acac)_2$ known as a catalyst for hydrogenation and polymerization is discussed based on the results of chemical, kinetic and physico-chemical (ESR, IR, UV, TEM, XRD) analysis. The formation of nanoscale cobalt metal particles is demonstrated. The particles are assumed to comprise the metal core and a stabilizing coating consisting of $AlEt_3$, $Et_2Al(acac)$ and the products of their transformations. The dependence of hydrogenation activity of the catalytic system on the Al/Co ratio passes through maximum, that is explained by changes of the composition of the nanoparticle stabilizing coating.

Keywords: Cobalt catalysts; Hydrogenation; Nanoscale cobalt metal

1. Introduction

The Ziegler type catalytic systems [1] based on the complexes of transition metals have found wide application as efficient catalysts for hydrogenation [2–5], isomerization [3–5], dimerization [6] and polymerization [1,7–13]. As early as in the 1960s, the hydrogenating activity of the catalytic systems formed from alkylaluminum and transition metal acetylacetonates was shown to exceed that of all up till then known forth row transition metal catalysts, both homogeneous and heterogeneous [2–5,14,15]. Ziegler suggested the formation of colloidal metals from cobalt and nickel acetylacetonates in the presence of large excess of trialkylaluminum [1], but Breslow and co-workers [2] and Kroll [16] did not confirm it. The state of oxidation of the catalytically active cobalt species formed in the system $AlEt_3$-$Co(acac)_{2,3}$ was assumed to be two [17] though another group of researchers suggested reduction of Co(2+) to Co(0) [18]. Therefore, such questions as homogeneous or microheterogeneous nature of these catalytic systems and degree of oxidation of the transition metal are still of vivid interest for researchers. Our earlier experimental data [19–21] have been interpreted from the viewpoint of formation of polynuclear complexes containing cobalt in a reduced state and organoaluminum compounds. Yet, the structure of these complexes was not discussed.

In continuation of the earlier spectroscopic studies of the problem [18,22–26] and to get more systematic knowledge on formation of the catalytically active species we present here a complex approach based on the use of gas evolution analysis, measurement of kinetics, IR, UV, ESR spectroscopy, transmission electron microscopy and X-ray diffraction analysis to the solutions of $AlEt_3$-$Co(acac)_{2,3}$ as well as to the precipitates of metals formed in the system.

2. Experimental

All operations were performed in an inert atmosphere of argon purified from the traces of dioxygen and moisture by successive passing over Ni-Cr catalyst at 400 °C, through tubes with silica and bubbling through toluene solution

* Corresponding author. Tel.: +7 39 525 11425; fax: +7 39 523 96046.
E-mail address: bagrat@irioch.irk.ru (L.O. Nindakova).

1381-1169/$ – see front matter © 2005 Elsevier B.V. All rights reserved.
doi:10.1016/j.molcata.2005.02.033

of $AlEt_3$. Reaction vessels were dried at 200–250 °C and cooled in dry boxes in argon atmosphere. Reaction vessels used under vacuum were dried by flame at a reduced pressure.

Toluene, benzene, decaline, heptane and hexane were purified by conventional procedures [27] and dried for 7 days over P_2O_5. Toluene and benzene were refluxed over Na/benzophenone for 8 h and distilled under dry argon directly before the experiments. Water contents in freshly distilled solvents was <0.8 mmol/L, that is, much less than the $AlEt_3$ concentration in most experiments (>10 mmol/L). Decaline and heptane for UV measurements were passed through silica column to remove the traces of aromatics, then degassed under vacuum and recondensed into ampoules with Na mirror.

Dihydrogen was purified from dioxygen by passing over Ni-Cr catalyst at 400 °C and dried by freezing at 77 K and passing through silica.

$AlEt_3$ was obtained from commercial 90–95% solutions in benzine (Red'kin experimental plant, Russia) by pumping off the solvent and distillation of $AlEt_3$ in vacuum (bp 48–49 °C/1 mmHg) and stored in sealed ampoules under dry argon. For gas evolution experiments, hydrogenation of alkenes, ESR and IR spectroscopic investigations freshly prepared 0.5 or 1 M solutions of $AlEt_3$ in hexane, benzene, or toluene were used. For UV spectroscopic studies, the distilled $AlEt_3$ was degassed under vacuum (10^{-3} mmHg) and divided in small portions (0.01–0.25 g) sealed in thin-wall glass beads.

Anhydrous cobalt bis- and tris-acetylacetonates were prepared according to [28], dried at 110 °C under vacuum to constant weight, crystallized from dry toluene and sublimed at a reduced pressure directly before use. Samples with different water contents [$Co(acac)_2 \cdot 0.5H_2O$ and $Co(acac)_2 \cdot 1.8H_2O$] were prepared by regulating the time of drying and calcination of the samples. The residual water in the samples was determined by thermogravimetric method on a MOM derivatograf (Hungary), the heating rate 5 °C/min.

2.1. Hydrogenation of alkenes

The reaction was performed in a vigorously agitated glass vessel placed on a shaker (300 swings/min). As was proved by special experiments the intensity of stirring of more than 250 swings/min does not affect the hydrogenation rate. The reactor made it possible to control dihydrogen consumption by measuring the drop of pressure in the system and to recover the pressure when it dropped by more than 20% of the initial value. The reactor was thrice evacuated and filled with dihydrogen and charged with 0.1–0.2 mmol of $Co(acac)_2$, 15–18 mL of solvent, 0.2–2.0 mmol of Et_3Al from the Schlenk tube. Then, it was plugged with stopper, dihydrogen pressure increased to 2 atm, 1–2 mL of olefin injected by syringe through the stopper, the shaker switched on and kinetic measurements were carried out.

2.2. Preparation of the samples for spectroscopic studies

ESR spectra were recorded at 77 K or at room temperature for 0.01–0.02 M solutions on a Rubin spectrometer or a SE/X-2542 instrument (both with 9.6 GHz working frequency) equipped with magnetometer. 2,2-Diphenyl-1-picrylhydrazyl was used as a standard ($g = 2.0037 \pm 0.0002$). The reaction between the components of the catalytic system was performed at room temperature in argon atmosphere in a vessel having a "sprout" for ESR measurements. The concentration of complexes was 10 mmol/L. To a vigorously stirred on a magnetic stirrer solution of 25.7–51.4 mg (0.1–0.2 mmol) of $Co(acac)_2$ in 8–10 mL of dry toluene in a flow of dry argon 0.2–2.0 mmol of $AlEt_3$ solution was added quickly all at once or dropwise (2–3 drops/s) from the Schlenk vessel. The rate of addition affects the intensity of the ESR signal of the Co(0) complex so that for quick addition a high concentration (up to 80–90% of the initial complex concentration) of the Co(0) complex was achieved whereas its dropwise addition led to low concentration of the Co(0) complex not exceeding 40%. For low-temperature measurements, the solution in the sprout was frozen with liquid nitrogen in 2–3 min after mixing of the reagents and the ESR spectra were registered. The concentration of the paramagnetic Co(0) complexes was estimated by comparing the integral intensities of the ESR spectra (doubly integrated ESR spectra) of the reaction mixture to those of the chloroform solution of paramagnetic complex $Cu(acac)_2$ at 77 K.

UV spectra were taken on a Specord UV–vis instrument in the range 50,000–28,000 cm^{-1}. The reactions were performed under vacuum (10^{-3} mmHg) in glass systems connected to quartz UV cell of 0.01 cm thickness. Concentration of Co complexes was 2 mmol/L. A specimen of $Co(acac)_3$, thin-wall glass bead with pure $AlEt_3$ and a plunger were placed into a glass vessel sealed to a quartz UV cell. The system was pumped out and 10 mL of a degassed solvent was recondenced into it from the ampoule with sodium metal mirror, the vessel with the cell was sealed out from the vacuum line and the UV spectrum of the initial compound was recorded. Then, the ampoule with $AlEt_3$ was broken with plunger, the solution was stirred and spectra were registered at specified time intervals.

FTIR spectra were recorded on a IFS-25 spectrometer in nujol. Nujol was pre-heated for 6 h in vacuum (80 °C/1 mmHg), degassed and stored under dry argon. The samples were prepared in a dry box filled with argon. Solutions of complexes and their mixtures ($C_{Co} = 25$ mmol/L) were prepared in a Schlenk tube in dry argon atmosphere, then transferred with a syringe into a preevacuated and filled with argon KBr cell (l 0.013 cm). Air-sensitive solid samples were prepared by removal of toluene under vacuum, washing the precipitate with dry hexane and drying under vacuum (30 °C/1 mmHg). Dry samples were sealed under argon and used for FTIR spectroscopy and X-ray diffraction analysis.

X-Ray diffraction analysis of solid precipitates was performed on a DRON-3M diffractometer, Cu Kα irradiation.

Transmission electron microscopy (TEM) was carried out on a BS-450 instrument with accelerating voltage 80 kV for samples obtained by deposition of the toluene solution of Et_3Al-$Co(acac)_2$ with Al/Co = 4 (C_{Co} 5 mmol/L) on a commercial grade copper carrier grid coated with carbon film (400 mesh) with subsequent removal of the solvent in the lock chamber. All experiments were performed with a minimal current of the electron beam sufficient for observation but excluding the possibility of melting and decomposition of the samples as well as their reduction to cobalt metal in TEM beams, as proved by repeated exposure of the object and comparison of the images.

2.3. Gas evolution

The reaction was performed in a 100 mL vessel equipped with a sprout with a vacuum valve. The vessel was evacuated, filled with argon, placed on a magnetic stirrer and under the flow of dry argon 0.257 g (1 mmol) of $Co(acac)_2$ was charged and dissolved in 20 mL of dry toluene (C_{Co} = 50 mmol/L). The reactor was connected to a Schlenk vessel containing $AlEt_3$ solution. The sprout was connected to a thermostated gas burette, then the gas flow was stopped and the required amount of $AlEt_3$ solution added (2–8 mL of 1 M solution). After the gas evolution was ceased the volume of the evolved gas was measured at 25 °C and recalculated to normal conditions (0 °C). The volume of the evolved gas was corrected to the solubility of its components in liquids $q = K'p$ with the use of the Henry coefficients at 25 °C: in toluene $K'(H_2)$ 5.223×10^{-7}, $K'(C_2H_6)$ 2.568×10^{-5}, $K'(C_2H_4)$ 1.737×10^{-5}, $K'(C_4H_{10})$ 1.238×10^{-5} and $K'(C_4H_8)$ 1.870×10^{-5} [29]; in water $K'(H_2)$ 1.780×10^{-8} [29], $K'(C_2H_6)$ 5.244×10^{-8} [29,30], $K'(C_2H_4)$ 1.293×10^{-7} and $K'(C_4H_{10})$ 3.458×10^{-8} mol/mol mmHg [29,30].

Al-C_2H_5 balance was performed for Al/Co = 4 as in [31] with due correction to the gas solubility in the solvents used, calculated from the the Henry coefficients given above.

Initially taken	12.0 mmol Al–C_2H_5
1. Evolved reaction gas + gas dissolved in toluene	2.1 mmol (76.2% ethane, 22.3% ethylene, 1% butane, 0.6% butenes, that corresponds to 2.2 mmol Al–C_2H_5 groups)
2. Condensate + hexane after washing	4.5 mmol Al–C_2H_5 (as ethane)
3. Protonolysis of wet precipitate	4.3 mmol Al–C_2H_5 (95.8% ethane, 4.2% ethylene)
Total balance 1 + 2 + 3	11.0 mmol Al–C_2H_5, i.e. 91.7% of the initially taken.

After drying 0.288 g of air-sensitive black powder was obtained. Elemental analysis corresponds to gross formula $CoAl_{1.9}C_{8.2}H_{13.9}O_{5.2}$.

GC analysis was performed on a LKhM-8D chromatograph with heat conductivity detector, carrier gas—dinitrogen or helium, columns 5 mm × 1 m filled with zeolite CaA, fraction 0.18–0.2 mm, temperature 20–50 °C. The composition of the gas mixture was calculated with taking into account the sensitivity coefficients *k* for the components [29], which are different for the two carrier gases.

2.4. Deuteration experiments

In a pre-evacuated and filled with dry argon vessel placed on a magnetic stirrer 1 mmol of $Co(acac)_2$ was dissolved in 16 mL of dry toluene and 4 mL of 1 M solution of $AlEt_3$ was added under the flow of argon. After 15 min, the vessel was equipped with a reflux condenser and the solution decomposed by addition of 5 mL of D_2O. The organic layer was immediately separated, washed with water, dried over P_2O_5 and distilled. The contents of $C_6H_5CH_2D$ was determined by ^1H NMR spectroscopy. For molar ratio Al/Co = 4, 0.15 molar% of deuterium was found, that corresponds to 0.283 mmol of deuterated toluene.

Elemental analysis of the precipitates was performed on a Finnigan CHN-analyzer (Italy). The content of metals was determined by the method of atomic adsorption spectroscopy on a Perkin-Elmer-403 instrument in the flame of propane-air (for cobalt) and acetylene-nitrous oxide (for aluminum).

2.5. Diethylaluminum acetylacetonate $Et_2Al(acac)$

To the solution of 55.2 mmol of $AlEt_3$ in 20 mL of purified decaline at −45 °C in argon atmosphere 5.4 mL of acetylacetone was added during 1 h. The mixture was stirred, allowed to warm to room temperature and distilled at 68–72 °C/3 mm Hg to afford light-yellow liquid, which was sealed in portions. Molecular mass determined by cryoscopy in benzene under dry argon was 310 ± 30. ^1H NMR spectrum was registered on a Varian-200 spectrometer in C_6D_6, δ, ppm: 0.53 q (4H, CH_2Al, *J* 8.2 Hz), 1.54 t (6H, $\underline{CH_3}CH_2$, *J* 8.2 Hz), 1.58 s (6H, CH_3CO), 4.95 s (1H, CH).

3. Results

3.1. Catalytic activity

The catalytic activity of the system formed from $AlEt_3$ (**1**) and $Co(acac)_2$ (**2**) in hydrogenation of olefins in toluene plotted against the Al/Co molar ratio in Fig. 1 passes through maximum. The position of the maximum depends on water contents in $Co(acac)_2 \cdot nH_2O$. For hydrogenation of styrene it lies at Al/Co = 4 for $n = 0$ and at Al/Co = 8 for $n = 1.8$. The amount of the precipitate formed in the system is also maximal at these Al/Co ratios. Presence of water also accelerates the rate of hydrogenation (96.4 mmol/L min for $n = 1.8$ versus 46.9 mmol/L min for $n = 0$). Existence of maxima on the plot of the catalytic activity versus Al/Co ratio was also found for systems $AlEt_3$-metal acetyl acetonates, which are active in stereoregular polymerization of acetylene [17]. For the system formed from $AlEt_3$ and $Co(acac)_3$ (**2a**) the catalytic activity is maximal at Al/Co = 3.

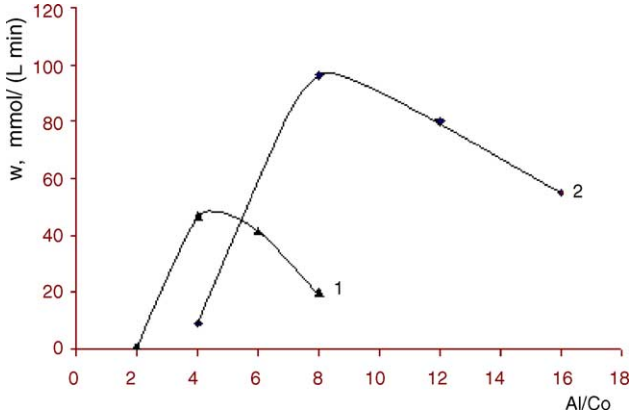

Fig. 1. Rate of hydrogenation of styrene in the system $AlEt_3$-$Co(acac)_2 \cdot nH_2O$ in toluene as a function of Al/Co ratio. $n = 0$ (1); $n = 1.8$ (2). C_{Co} 10 mmol/L, $C_{styrene} = 1$ mol/L.

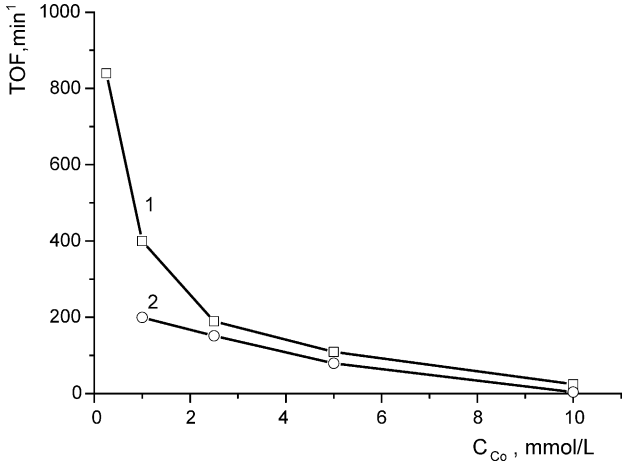

Fig. 2. Catalyst turnover frequency (TOF) in hydrogenation of 1-hexene as a function of cobalt concentration for optimal Al/Co ratios (1—in heptane; 2—in toluene).

The results of a detailed study of kinetic regularities of the olefin hydrogenation on the catalytic system $AlEt_3$-$Co(acac)_2$ as a function of Al/Co ratio, the solvent nature and the amount of crystallization water in $Co(acac)_2$ were discussed in our earlier works [14,15,19–21]. The turnover frequencies (TOF) of the catalyst for hydrogenation of olefins in toluene at normal pressure, 20 °C and $C_{Co} = 2.5$ mmol/L are as follows: 100 min^{-1} (styrene) and 150 min^{-1} (1-hexene).

The maximum values of activity of the Et_3Al-$Co(acac)_3$ system were obtained for hydrogenation of 1-hexene in heptane at low concentrations of the initial Co(2+) complex (Table 1). For Al/Co = 50, the TOF of the catalyst in heptane (run 2) calculated from the initial rates of hydrogenation is 17 times as high as that in toluene (run 4).

Fig. 2 shows the dependence of the catalyst turnover frequency on cobalt concentration for hydrogenation of 1-hexene in toluene and heptane at optimal Al/Co ratios. As can be seen, TOF decreases with cobalt concentration. Since for actual homogeneous catalyst the activity does not depend on C_{Co}, the obtained results cannot be rationalized from the viewpoint of homogeneity of the system. A similar increase of the catalyst activity at low concentration of the metal was observed for catalysis of hydrogenation reactions by nanoclusters, and it was assigned to lower probability of bimolecular aggregation of particles [32].

3.2. Spectroscopic studies

Mixing of **1** with **2** ($C_{Co} = 5$ mmol/L, Al/Co = 2, 8) leads to visually homogeneous dark-brown solution stored under argon atmosphere for months without apparent changes. For Al/Co = 4, the solution is not transparent and after a week the precipitate is formed. The presence of crystallization water in **2** immediately results in the formation of a black precipitate, its yield increasing with water contents in the initial $Co(acac)_2$. In all cases gas evolution is observed. The results discussed below refer to anhydrous $Co(acac)_2$.

3.2.1. UV spectroscopy

UV and ESR studies of the system Et_3Al-$Co(acac)_{2,3}$ was the subject of our earlier works [19,21–24]. Here, they are briefly summarized in order to compare to the results obtained by other methods.

When **2a** reacts with 3 equivalents of **1**, the intensity of absorption bands of **2a** at 44,000 cm^{-1} (ν_1) and 39,000 cm^{-1} (ν_2) in decaline decreases and a new band ν_3 of $Al(acac)_3$ **3** appears. For Al/Co = 6–10 new bands at 37,300 cm^{-1} (ν_4) and 32,500 cm^{-1} (ν_5) appear which belong to $Et_2Al(acac)$ **4**, the ratio of concentrations [**4**]/[**3**] = 4. For Al/Co = 10–20 the spectrum shows only the bands of **4**. When two equivalents of durene are introduced into the system with Al/Co = 6, after 2 min both **3** and **4** appear with the [**4**]/[**3**] = 10. For Al/Co = 10 only **4** is observed, that is indicative of its

Table 1
Hydrogenation of 1-hexene on $Co(acac)_3$-$AlEt_3$ in heptane ($C_{olefin} = 0.4$ mol/L)

Run	C_{Co} (mmol/L)	Al/Co	TOF (min^{-1})
1	0.15	100	310
2	0.25	100	357
3	0.25	50	850
4	0.25	25	230
5[a]	0.25	50	50
6	0.5	25	200

[a] In toluene.

stabilization in the presence of Co and arene. Therefore, the ratio of the products of the reaction of **2a** with **1** is governed by Al/Co molar ratio. Compound **4** was prepared independently and its UV spectrum showed the same bands ν_4 and ν_5, that proves the validity of the assignment. Cryoscopic measurements of molecular mass of **4** showed it to exist in benzene as a dimer ($M = 310 \pm 30$). This fact in conjunction with the presence of two bands in the UV spectrum of **4** in decaline allows to assume that **4** is dimeric in decaline as well.

3.2.2. ESR spectroscopy

Solution of **2** in toluene (C_{Co} = 10 mmol/L) does not show ESR signals. Addition of **1** (Al/Co = 3–5) into the system results in evolution of gaseous products (ethane, ethylene, dihydrogen, butenes) and appearing of two signals of low intensity in the ESR spectrum at room temperature: the septet signal I (g = 2.004; a(H) = 1.2 mT) with binomial distribution of the line intensities (1:6:15:20:15:6:1) [33] and a broad singlet II (g = 2.26; $\Delta H \approx 80$ mT), similar to that observed by Misono for the system $Co(acac)_3$-$AlEt_3$ [18]. Signal I, apparently, belongs to dianion radicals of acetylacetone whose formation was proved for the system $Co(acac)_2$–RMgBr [34], whereas signal II is caused by ferromagnetic cobalt species (Fig. 3).

At 77 K an intense signal III appears (Fig. 3, $g_{||}$ 2.344; $g_{\perp}$ 2.054; $A_{||}^{Co}$ 6.08 mT; $A_{\perp}^{Co}$ 1.48 mT) along with a weak signal II existing also at a low temperature. With anhydrous $Co(acac)_2$ at C_{Co} = 5–10 mmol/L and Al/Co = 5, the intensity of signal III reaches its maximum after 2–3 min corresponding to 80–90% of the initial $Co(acac)_2$ concentration, then decreases with the half-life ca. 30 min. The intensity of signal II as a function of Al/Co passes through maximum at Al/Co = 1. The relative intensity of signal II increases with water contents.

Noteworthy, the maximum intensity of signal III depends on the rate of addition of **1** into the toluene solution of **2**: the above behavior is observed when **1** is added as quick as possible, whereas a dropwise addition leads to the intensity corresponding to only ~40% of the initial concentration of **2**. Signal II has minimum intensity, close to zero, in the case of anhydrous **2** at Al/Co = 4 but its intensity grows with water contents in the system.

Signal III is observed only in the presence of arenes in the systems containing Co complexes with oxygen-containing ligands (acetylacetonates, acetates, aminoacid salts) and organometal compounds of Al, Mg, Na, or Li, as well as in systems formed by cobalt halides and Et_2O or alkylacetates [35–38]. The parameters of signal III were shown to depend on the number and location of alkyl groups in the arene molecule and the degree of branching at the α-carbon atom in the alkyl group of organometal compound, and do not depend on the nature of the metal (Al, Mg, Li) [35]. The experimental data comply with the formation of $[(\eta^6\text{-ArH})CoR(acacAlR_2)]^- R_2Al^+$ at-complex having in the first coordination sphere of Co the arene molecule, α-carbon atom of ethyl group from **1** and the ethereal oxygen atom from the acetylacetonate anion [36,38].

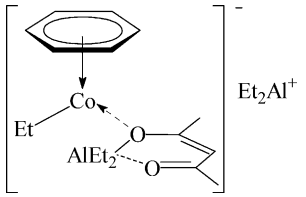

Signal III belongs just to this at-complex. Fig. 4 shows time dependence of the relative intensity of signals II and III. The initial intensity of signal III for the system prepared in dihydrogen atmosphere (curve 1) is ca. half of that in argon (curve 3), and the spectrum also contains signal II. If the system prepared in argon is treated after 1–2 min with dihydrogen, the intensity of signals II and III becomes equal to their intensity in the system originally prepared in dihydrogen. Yet, the rates of depletion of signal III in argon and in dihydrogen are about the same.

Introduction of 1-hexene into the system showing signal III leads to a decrease of its intensity (three times after 20 min) and appearance of a new signal IV (Fig. 3). The

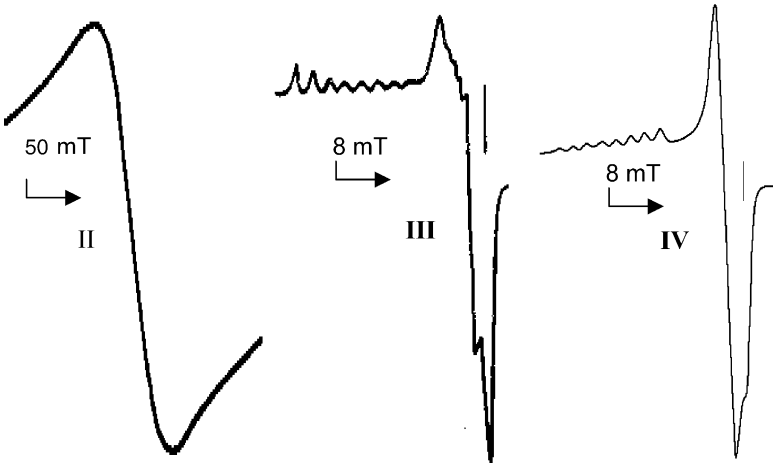

Fig. 3. ESR signals in the system $AlEt_3$-$Co(acac)_2$: ferromagnetic Co(0) complex (II); complex $[(\eta^6\text{-}C_6H_6)EtCo(acacAlEt_2)]^- AlEt_2^+$ (III); complex $[\eta^6\text{-}C_6H_6)Co(1\text{-hexene})(acacAlR_2)]$ (IV).

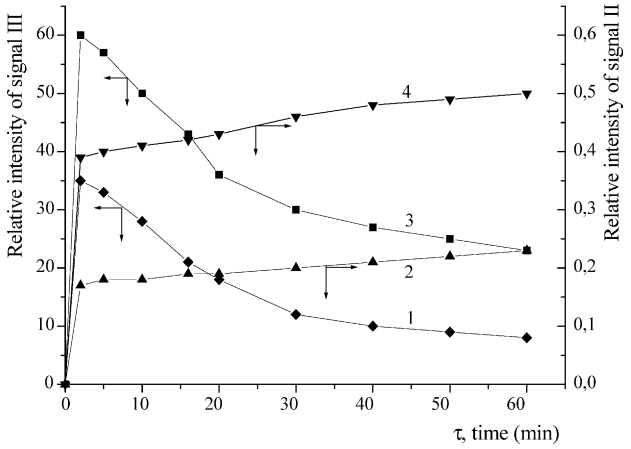

Fig. 4. Time dependence of the relative intensity of signals II and III. 1—signal III in dihydrogen; 2—signal II in argon; 3—signal III in argon; 4—signal II in dihydrogen.

latter belongs to π-complex of Co(0) formed by substitution of triethylaluminum from the coordination sphere of cobalt in the above at-complex by olefin to form complex $[\eta^6\text{-ArH})Co(CH_2{=}CHR')(acacAlR_2)]$. Introduction of dihydrogen initiates the process of hydrogenation of 1-hexene and after 2 min signal IV disappears and the rate of hydrogenation reaches its maximum value. This is a corroboration of the fact that alkene–arene Co(0) complexes are the precursors of the true catalyst of hydrogenation. At the same time, the integral intensity of signal II sharply increases and reaches the value exceeding the value characteristic for the initial cobalt concentration. The observed increase of paramagnetism may be due to strong exchange interaction between the reduced cobalt particles [20]. Therefore, during the process of hydrogenation of olefins a transformation of the labile Co(0) complexes into ferromagnetic species showing signal II occurs. The latter species also act as catalysts for alkene hydrogenation. In the light of these data the decrease of signal III and increase of signal II upon the treatment of the system formed in argon with dihydrogen is explained by hydrogenation of ethylene and butenes on Co(0) that brings about the formation of ferromagnetic species. Hence, Co(0) complexes responsible for signal III virtually do not interact with dihydrogen whereas the olefin complexes showing signal IV are very reactive with respect to dihydrogen and it is these complexes which catalyze the process of hydrogenation in the initial step.

From the data of the ESR and UV spectroscopy one can conclude that signal III observed in the ESR spectra of the system $Et_3Al\text{-}Co(acac)_{2,3}$, on the one hand, and the absorption bands of **4** in the UV spectra of the same system stabilized in the presence of arene and cobalt, on the other hand, characterize one and the same Co(0) at-complex $[(\eta^6\text{-ArH})CoR(acacAlR_2)]^-AlR_2^+$ of the structure depicted above

3.2.3. FTIR spectroscopy

FTIR study of the system $AlEt_3\text{-}Co(acac)_2$ in benzene solutions showed that for Al/Co = 2–8 the acetylacetonate groups are transferred from Co to Al to afford aluminum acetylacetonates. For Al/Co = 2 after 20 min the intensity of absorption bands at 1592 and 1520 cm^{-1} in **2**, characterizing mixed vibrations $[\nu(C{=}O) + \nu(C{=}C)]$ and $[\nu(C{=}C) + \nu(C{=}O)]$ [39] drops and new bands appear at 1596 and 1530 cm^{-1} (Fig. 5). The intensity of the band of mixed vibrations $[\nu(C{-}Me) + \nu(C{=}C)]$ at 1259 cm^{-1} in **2** substantially decreases and a new band belonging to aluminum acetylacetonate complex appears at 1291 cm^{-1}. The spectrum, however, is not a superposition of those for **2** and **4** since the band at 1259 cm^{-1} suffers high-frequency shift to 1264 cm^{-1} and the band of $AlEt_3$ at 1228 cm^{-1} is absent (Table 2). A high-frequency shift is indicative of the ligand binding to a more strong Lewis acid (Al as compared to Co). The content of **3** which shows the main bands at 1590, 1523, 1291 and 485 cm^{-1} and the ratio of intensities $\delta(Al{-}O)/\nu[(C{=}O) + \nu(C{=}C)]$ of 0.5, is small since this ratio

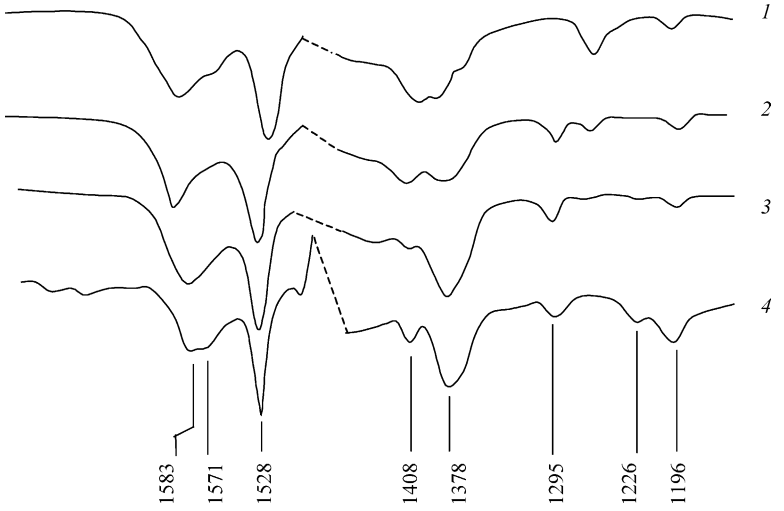

Fig. 5. FTIR spectra of $Et_3Al\text{-}Co(acac)_n$ in benzene (C_{Co} 25 mmol/L): $Co(acac)_2$ (1); Al/Co = 2, 20 min (2); Al/Co = 4, 20 min (3); Al/Co = 8, 20 min (4).

Table 2
FTIR spectra of Co and Al acetylacetonates and $AlEt_3$-$Co(acac)_2$ in benzene (C_{Co} = 25 mmol/L)

Species, Al/Co, time	ν(C=O)	ν(C=C)	ν(C=C) + δ(C–H)	ν(C–CH_3) + ν(C=C)	δ(Al–C–H) ν(C–CH_3)	δAl–O–C	δ(O–Al–O)
$Co(acac)_2$	1592	1520	1399, 1383, 1365	1259	1197		465[a]
$Al(acac)_3$	1590	1523	1390	1291	1186		485, 415
$AlEt_3$			1401, 1376		1228, 1196		
$AlEt_2(acac)$	1585	1530	1408, 1380	1295	1218, 1187		485 w
$Co(acac)_2$-$AlEt_3$, 2, 20 min	1596	1530	1408, 1381	1291, 1264	1193		493, 464
$Co(acac)_2$-$AlEt_3$, 2, 210 min	1598	1531	1408, 1393	1288, 1264	1190		493, 464
$Co(acac)_2$-$AlEt_3$, 4, 20 min	1587 1571sh	1529	1408, 1378	1295	1225, 1193	1100	493, 465
$Co(acac)_2$-$AlEt_3$, 8, 20 min	1585, 1574	1530	1408, 1378, 1324	1295	1226, 1197	1100, 1056	480, 465
$Co(acac)_2$-$AlEt_3$, 8, 135 min	1585, 1574	1530	1408, 1378, 1324	1295	1226, 1197	1100, 1056	480, 465

[a] ν(Co–O) + ν(C–CH_3) [23].

is 0.14 after 20 min and after 210 min it drops to 0.07, that is close to 0.05 found for **4**.

For Al/Co = 4 after 20 min the absorption bands [ν(C=O) + ν(C=C)], [ν(C=C) + ν(C=O)] and [ν(C–Me) + ν(C=C)] are observed at 1587, 1529 and 1295 cm^{-1}, respectively, that coincides with the set of absorption bands for **4** (Table 2). The spectrum for Al/Co = 8 after 20 min is similar to that for Al/Co = 4, except for the increase of the relative intensity of the shoulder band at 1571 cm^{-1}. In addition, the intensity of the band δ(AlCH) at 1196 cm^{-1} increases and a band ν(AlOC) at 1056 cm^{-1} appears. In the region of the Me–O stretching vibrations three bands of equal intensity appear at 480 and 465 cm^{-1}. All these observations are consistent with transformations in Scheme 1.

Structure **6** is consistent with the appearance and growth of the band ν(AlOC) at 1056 cm^{-1}. Formation of **7** by addition of another molecule of **1** to **6** is also possible. The content of **6** and **7** is apparently small and the main part of acetylacetonate groups exist in the chelate form (for Al/Co = 4–8 in the form of compound **5**). The ability of the O,O-coordinated acetylacetonate ligands to form O-complexes with additional O → metal bond with various metals is well known [40]. Note that reduction of $Pt(acac)_2$ with $AlMe_3$ leads to platinum nanoparticles coated by compounds of the type **7** [31]. Probably, the addition of $AlMe_3$ to $Me_2Al(acac)$ proceeds more easily than that of **1** to **4**.

Thus, the results of the IR spectroscopy show that in the catalytic system $AlEt_3$-$Co(acac)_2$ at Al/Co = 4 and 8 the formation of $Et_2Al(acac)$ (**4**) occurs as well as the products of its reaction with excess $AlEt_3$, namely **5**, **6** and **7**.

3.2.4. Transmission electron microscopy

Fig. 6 shows TEM images obtained for the sample prepared from the toluene solution of the system $AlEt_3$-$Co(acac)_2$ at Al/Co = 4 (C_{Co} = 5 mmol/L). The sample contains mainly rounded cobalt metal particles with diameter predominantly from 2 to 5 nm, which contain organic phase. Larger particles of 10–50 nm deposited from the solution consist of smaller ones with the basic size of ~5 nm and also contain organic phase. The histogram for distribution of small particles in size shows two distinct maxima at 2.6 and 5.0 nm (Fig. 7).

Therefore, interaction of the components of the catalytic system Et_3Al-$Co(acac)_2$ results in formation of nanoscale cobalt metal particles dispersed in toluene and, apparently, stabilized by the formed organoaluminum compounds and/or solvent.

3.3. Gas evolution

The main amount of gaseous products upon mixing $AlEt_3$ with $Co(acac)_2$ in toluene is evolved in the first 5–6 min. The yield of the gas increases with molar ratio Al/Co and at Al/Co = 8 reaches 3.4. The evolved gas contains ethane, ethylene, butane and isomeric butenes (Table 3).

Evolution of more than 2 mol of gaseous products per 1 mol of cobalt and non-stoichiometric ethane/ethylene ratio

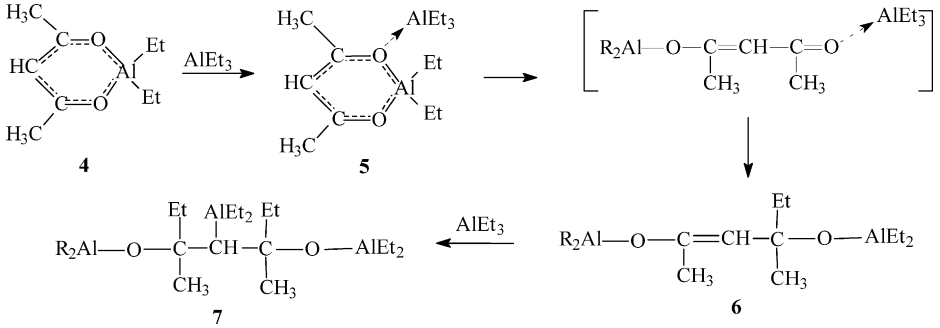

Scheme 1.

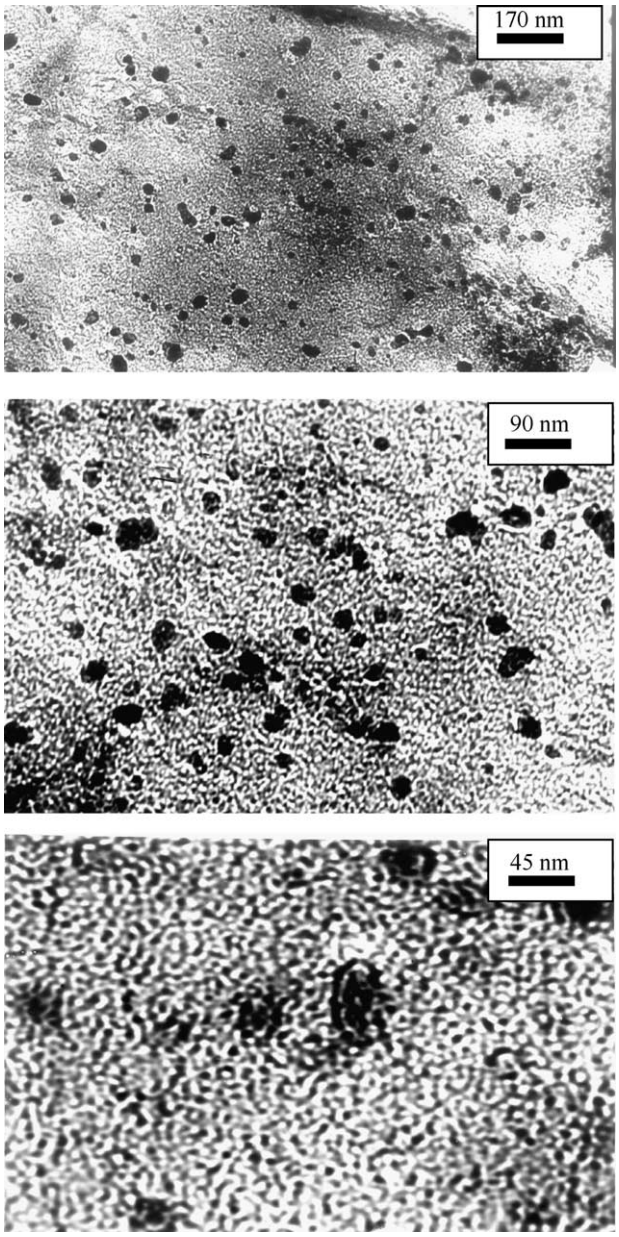

Fig. 6. TEM images of Co nanoparticles formed in toluene solution of $Co(acac)_2$-$AlEt_3$ (C_{Co} 5 mmol/L, Al/Co = 4).

Table 3
Yield and composition of effluent gases in reaction of $Co(acac)_2$ with Et_3Al (toluene, C_{Co} 50 mmol/L)

Al/Co	Mol gas/mol Co (mol Et/mol Co)	Composition (%)			
		Ethane	Ethylene	Butane	Butenes
2	1.54 (1.58)	89.8	7.8	2.4	0.04
4	2.12 (2.16)	76.0	22.3	1.1	0.6
8[a]	3.42 (3.54)	83.7	13	2.2	1.1

[a] C_{Co} = 10 mmol/L.

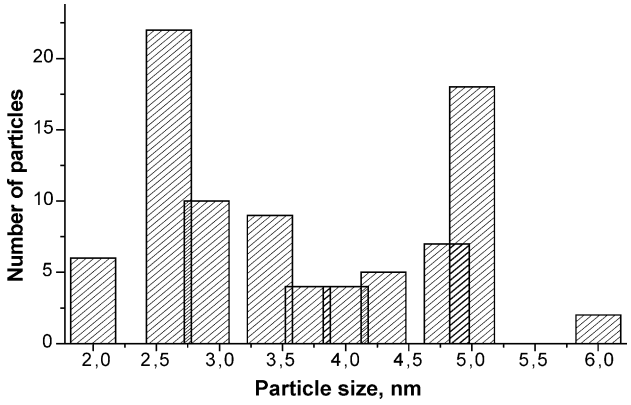

Fig. 7. Size distribution of Co particles formed in the system $Co(acac)_2$-$4AlEt_3$ in toluene.

suggests that the reaction under consideration does not come to simple reduction of Co(2+) to Co(0) according to Eq. (1).

$$Co(acac)_2 + 2Et_3Al \rightarrow Co(O) + 2Et_2Al(acac) + C_2H_6 + C_2H_4 \quad (1)$$

Reaction similar to (1) was assumed in [18,41], where the authors studied decomposition of organocobalt compounds to free radicals. Misono and co-workers [18] have studied gas evolution in the system $AlEt_3$-$Co(acac)_3$ only for Al/Co ratios from 0.5 to 1.5 under the conditions of gradual addition of **1** into $Co(acac)_3$ solution and vice versa, addition of $Co(acac)_3$ into the solution of **1**. They have shown that under the conditions of gradual addition of $AlEt_3$ the reduction of Co(3+) into Co(0) proceeds via an intermediate formation of $Co(acac)_2$, whereas all at once addition of $Co(acac)_3$ into the solution of **1** affords Co(0) immediately. The amount of the gas evolved reaches ca. 70% of the theory and it contains ethane and ethylene. Prince and Weiss [41] have studied the system $AlEt_3$-$CoCl_2$ also for low Al/Co ratio (0.6) and showed that the amount of ethylene formed reaches 25–30%. According to [26], for equimolar ratio of $Co(acac)_3$ and $AlMe_3$ along with formation of gaseous products (methane 77%, ethane 21% and ethylene) cobalt metal is formed though the authors did not analyze the precipitate in detail. Therefore, these results were obtained for the Al/Co ratios lying beyond the interval in which the system demonstrates the highest activity in the hydrogenation reaction; moreover, the authors did not take into account the solubility of gases in the liquids used.

According to [42], the ratio of the rates of disproportionation and recombination of ethyl radicals (r_D/r_C) in toluene is equal to 0.167 that means that a high excess of dimeric products (butane, butenes) over the monomeric ones (ethane, ethylene) should be observed. However, we have found that in the presence of styrene, which quantitatively traps free radicals, the yield and composition of gaseous products do not change, that means that the process occurs in the metal coordination sphere without emerging free radicals to the bulk.

Formation of ethane and ethylene by the disproportionation reaction proceeds via intermediate **8** by route ***b*** in

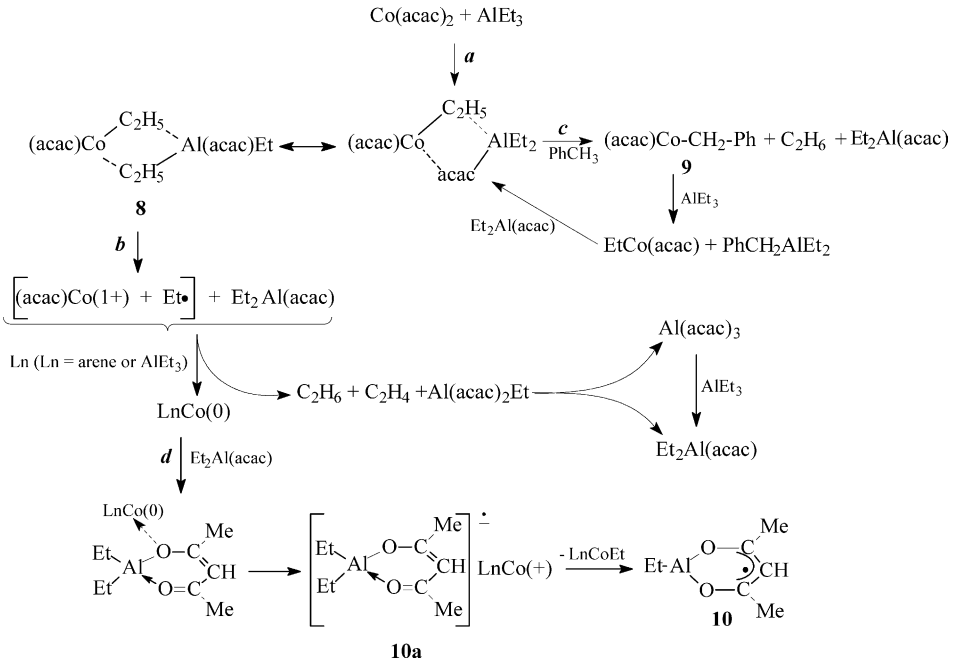

Scheme 2.

Scheme 2, which does not explain, however, the predominance of ethane over ethylene. The excess of ethane over ethylene is indicative of the presence of additional sources of hydrogen in the system, which may be as follows:

(a) Abstraction of hydrogen atom from the solvent with the formation of Co(2+) benzyl derivative **9** (route ***c***, Scheme 1), that is proved by the presence of deuterated toluene (0.28 mol of toluene-d_1 per 1 mol of Co) in the reaction mixture after its quenching with D_2O. The comparison of the amount of deuterated toluene and the gas evolved shows that about 13% of ethane is formed by hydrogen abstraction from the solvent. The benzyl derivatives of Co(1+) or Co(2+) (like **9**) can react with **1** to form additional amount of gaseous products.

(b) Abstraction of hydrogen atom from $AlEt_3$ by ethyl radical with the formation of structures $Et_2AlCH_2CH_2AlEt_2$. This may also explain a "lack" of ethylene in the gas phase. Wilke and co-workers [43] have shown by the use of deuterium label that upon decomposition of complexes L_nNiCH_3 methane is formed both due to abstraction of hydrogen atom from **1** by methyl radical and the reaction of methyl radical with toluene. Decomposition of $AlEt_3$ with $TiCl_4$ was shown to include abstraction of hydrogen atom from the alkyl group bound to metal [44].

(c) Oligomerization of ethylene. There is no balance of the total amount of ethyl groups formed by the reaction between the components and after decomposition of the system with water. In particular, the amount of ethyl groups bound to Al and released upon hydrolysis (97.6% ethane and 2.4% ethylene) for Al/Co = 4 amounts to 9.1 mol/mol Co (75.8% of the initial contents). The lack of ethyl groups equal to 0.74 mol/mol Co can be explained both by oligomerization of ethylene and addition of **1** to unsaturated bonds in **4**.

(d) Decomposition of **1** on Co(0) complexes with the formation of aluminum hydrides or Al(0). Thus, when the toluene solution of [$Co(acac)_2$ + 8 $AlEt_3$] was stored during 48 h in argon atmosphere and then decomposed with aqueous alkali solution the analysis of the gas phase showed the presence of 2.6% of dihydrogen along with 94.8% of ethane and 2.6% of ethylene. Dihydrogen could form due to hydrolysis of aluminum hydride or Al(0), its amount corresponded to 1.21% of Al(0) or 0.8% of Al–H.

All these routes contribute with different weights into the total process of gas formation, so, the whole process cannot be described by a unified stoichiometrically balanced reaction. However, to illustrate how Eq. (1) can be modified by taking into account the involvement of solvent (toluene) for specific Al/Co ratio (equal to four for the most catalytically active system) below is given Eq. (2) demonstrating the predominance of ethane over ethylene as well as the presence of butane due to formation of organoaluminum compounds like $Et_2Al(acac)\cdot AlEt_3$, $Et_2AlC_7H_7$ and $Et_2AlCH_2CH_2AlEt_2$:

$$4Co(acac)_2 + 16AlEt_3 + C_7H_8 \rightarrow 4Co(0) + 3Et_2Al(acac) + 5Et_2Al(acac)\cdot AlEt_3 + Et_2AlC_7H_7 + Et_2AlCH_2CH_2AlEt_2 + 6C_2H_6 + 4C_2H_4 \quad (2)$$

Other aforementioned routes altering the composition of the mixture of gases evolved could be allowed for in a similar way provided that their relative contribution was known.

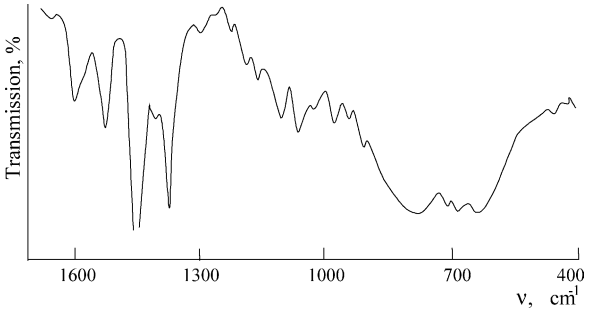

Fig. 8. FTIR spectrum of precipitate isolated from the system $Co(acac)_2$-$8AlEt_3$ in nujol.

A low-intense ESR septet signal detected in the catalytic system $AlEt_3$-$Co(acac)_2$ at room temperature belongs to radical **10** [34] which can be formed by route ***d*** in Scheme 2. Single electron transfer from the reduced metal to the chelate ring of the acetylacetonate ligand is followed by formation of relatively stable **10** and Co(1+). Reduction of the latter with $AlEt_3$ will also afford additional gaseous products. Reaction of **10** with ethyl radical leads again to Et_2Alacac. It is pertinent to note that routes ***c*** and ***d*** are not the main ones but lead to by-products.

Therefore, formation of more than 2 mol of gaseous products per one mol of Co is the result of consecutive transformations of unstable alkyl and hydride derivatives of Co(2+) and Co(1+) under the action of **1**.

3.4. Composition and nature of solids deposited from the catalytic system

To establish the composition of precipitates formed in the catalytic system Et_3Al-$Co(acac)_2$ at Al/Co = 2, 4 and 8, they were isolated under dioxygen- and moisture-free conditions, washed with hexane and dried.

3.4.1. FTIR spectroscopy

Like the FTIR spectra of solutions, the FTIR spectra of the precipitates (Fig. 8) also show characteristic bands of acetylacetone chelated to aluminum (1600, 1530, 1296–1301 cm^{-1}). An intense broad band characteristic of Al–O vibrations is observed in the 600–800 cm^{-1} region, as well as absorption bands of Al–C (1193, 694 cm^{-1}) and Al–O–C (1073, 1112 cm^{-1}).

Comparison of these bands to those in the individual aluminum compounds {$Et_2Al(acac)$ (**4**) in Table 2 and alumoxanes [13]} suggests that the precipitates contain **4**, alumoxanes with AlOAl bond (570–780 cm^{-1}) and a small amount of $(EtO)_2Al(acac)$ (800 cm^{-1}) which may be formed by partial oxidation of **4** during the sample preparation. Note that **3** is hardly present in the samples, because for it the ratio of intensities $\nu(Al–O)/[\nu(C{=}O) + \nu(C{=}C)]$ is 0.5 whereas in all samples showing the Al–O absorption band this ratio does not exceed 0.06.

3.4.2. XRD phase analysis

The precipitates isolated from the catalytic system at Al/Co = 4 as described above are roentgen amorphous (highly disperse) and show broaden diffraction lines [45]. After calcination in argon at 450 °C for 4 h, the samples become more crystalline and four distinct maxima appear with *d*/*n* 2.040 (100), 1.773 (80), 1.253 (50), 1.07 (50), which belong to elemental cobalt metal in cubic modification (β-Co) [45]. The size of the particles calculated by the Seljakov–Shereer formula [46] is ca. 10 nm. Additional calcination of the sample at 500 °C for 5 h leads to further narrowing of the lines and the calculated size of the particles increases to 19 nm.

3.4.3. Elemental analysis

Elemental analysis shows the presence of Co and Al in the precipitates, the Al/Co molar ratio being close to 2 (1.88–2.2). As can be seen from Table 4, the content of Co (17.7–18.4%), Al (16.1–17.9%), C and H as well as the ratios between the elements for the samples isolated at Al/Co 4 or 8 and after hydrogenation of 1-hexene are close.

Comparison of the element ratios in our samples to those for organoaluminum compounds given in Table 4 clearly illustrates that the composition of our samples is close to oligomeric alumoxanes (*n* = 4–5). Probably, the excess of **1** and **4**, which are not adsorbed on the surface of the Co metal particles, is washed out by hexane (see Section 2), and in addition, $Et_2Al(acac)$ and **1** are partly hydrolyzed.

Table 4
Elemental composition of precipitates isolated from system $AlEt_3$-$Co(acac)_2$ in toluene

Sample, Al/Co	Element ratio (mol/mol)				Formula
	Al/Co	C/Al	O/Al	H/C	
2	0.87	7.59	4.3	1.6	$Co[Al_2C_{15.2}H_{24.4}O_{8.6}]_{0.44}$
4	1.88	4.35	3.1	1.70	$Co[Al_2C_{8.7}H_{14.8}O_{5.5}]_{0.94}$
8	2.2	4.23	2.39	1.99	$Co[Al_2C_{8.5}H_{16.8}O_{4.8}]_{1.1}$
After hydrogenation, 4	2.12	3.67	3.09	2.13	$Co[Al_2C_{7.34}H_{15.68}O_{6.2}]_{1.06}$
$[Et_2Al(acac)]_2$	–	9	2	1.89	$Al_2C_{18}H_{34}O_4$
Alumoxane, *m* = 4[a]	–	6	2.75	1.58	$Al_4C_{24}H_{38}O_{11}$
Alumoxane, *m* = 5[a]	–	4.8	2.9	1.55	$Al_5C_{29}H_{45}O_{14}$

[a] *m* is the degree of oligomerization.

4. Discussion

The above information on the catalytically active species formation in the system Et_3Al-$Co(acac)_n$ ($n = 2, 3$) can be summarized as follows.

Judged from the ESR data the interaction of the catalytic system components in toluene in argon atmosphere leads to Co(0) arene complexes in concentrations comparable to that of the initial cobalt acetylacetonate. In the argon or hydrogen atmosphere these complexes eventually give rise to ferromagnetic structures as proved by appearing signal II in the ESR spectrum. The TEM images of the catalytic system prepared in argon show nanoparticles of 2.5–5 nm size, which, in turn, agglomerate to form secondary structures. It is reasonable to suggest that unstable arene Co(0) complexes are the precursors of nanoparticles with the core consisting most probably of cobalt atoms [47]. The largest of the latters or their agglomerates are responsible for signal II in the ESR spectrum. According to the ESR data, under the conditions of hydrogenation the maximum concentration of ferromagnetic cobalt is rapidly achieved.

Formation of ferromagnetic cobalt particles is apparently caused by aggregation and ordering of paramagnetic cobalt particles. The critical one-domain size for cobalt particles with one-axis anisotropy is 20–25 nm [48]. The maximum size of superparamagnetic Co particles determined by measuring the saturation and residual magnetization in systems containing particles of average size 10–15 nm is 6.4 nm [49]. In our case, the initially formed Co particles are of 2.5–5 nm size. Apparently, the observed ferromagnetism in the system is due to larger aglomerates of >10 nm size since the maximum intensity of signal II is followed by formation of a precipitate.

The surface of nanoparticles is always coated by a shelter of light atoms decreasing their surface energy and preventing their instant agglomeration [50]. On the other hand, electrostatic stabilization of nanoparticles is achieved by coordination of anionic or basic neutral ligands to the coordinatively unsaturated metal atoms on the surface of the metal particles [32]. In our case the role of such ligands can be played by chelate acetylacetonate derivatives of alkylaluminum, compounds **4** and **1**, and the products of their transformations, as well as by toluene. This is supported by the fact that the precursors of nanoparticles, Co(0) complexes, are stabilized by the molecules of arene, **1** and **4** (see Section 3.2.2). The structure of the colloidal particle can be conceived as a nucleus of cobalt metal coated by molecules of toluene, **1**, **4** and the products of the reaction of the latter with **1**, such as **5**, **6** or **7** [as illustrated in Fig. 9 for $AlEt_3$ and $Et_2Al(acac)$ ligands], the ratio between the coating components being determined by the excess of **1** in the system.

For Al/Co = 2, that is, when the catalyst is non-active (Fig. 1), the IR spectroscopy data show the formation of **4**, which under the conditions of virtually complete absence of free $AlEt_3$, apparently, acts as a stabilizer of the colloidal particles.

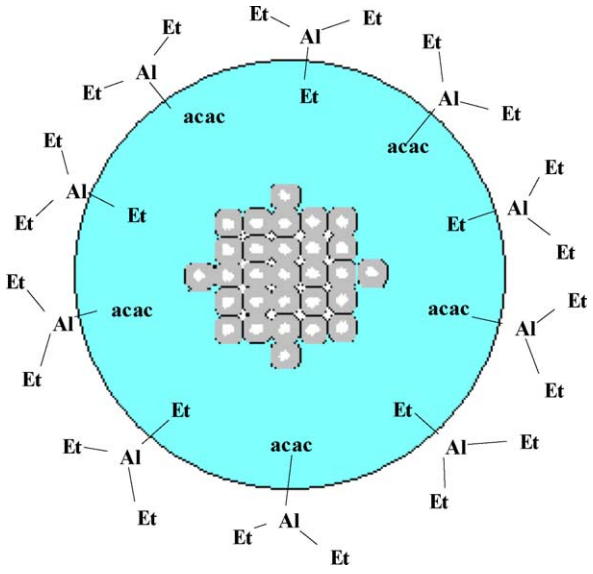

Fig. 9. Cobalt nanoparticle stabilized by organoaluminum coating.

Increase of Al/Co ratio to 4 results in coordination of **4** to the excess molecules of **1** to form **5** and **6**, which are less strongly bound to the surface of the particles. Remarkably, it is with this Al/Co ratio when consolidation of the colloidal particles in the system $AlEt_3$-$Co(acac)_2$ prepared in anhydrous solvents under dry argon occurs as a result of a lower ability of the protecting coating to prevent their aggregation. Simultaneously, it is with this Al/Co ratio when the highest catalytic activity in hydrogenation is observed (Fig. 1) since **5**, **6** and **7** are easily replaced by olefin. Thus, both the catalytic activity and aggregation of particles are determined by the presence of molecules weakly bound to the nucleus surface and readily replaced by the olefin molecules. Probably, the ease of replacement decreases in the order: arene > **7** > **6** > **5** > **4** > **1**.

For large Al/Co ratios (≥8), no precipitate is formed even after several weeks. In this case, the protecting coating consists mainly of $AlEt_3$ molecules, which, on the one hand, prevent aggregation, and on the other hand, hamper coordination of olefin leading to a sharp decrease or complete absence of the catalytic activity (Fig. 1). That AlR_3 molecules are apt to strong binding with metal core is proved by Bönnemann who elaborated the method of synthesis of nanoscale Co with stable magnetic properties and narrow size distribution by thermolysis of $Co_2(CO)_8$ in the presence of Al(*i*-Bu)$_3$ [51] and Pt nanoparticle networks by reduction of $Pt(acac)_2$ with $AlMe_3$ [52].

Presence of crystallization water in the catalytic system $AlEt_3$-$Co(acac)_2 \cdot nH_2O$ also changes the structure of the protecting coating. Part of Al–C bonds in **1** and **4** is hydrolyzed to form groups AlOH capable of hydrogen bonding, alumoxanes $R_2AlOAlR_2$, or acetylacetonate derivatives of alkylalumoxanes (acac)EtAlOAlR(acac) and their oligomers. This may facilitate aggregation of the nanoscale colloidal Co metal particles into larger agglomerates. As a result, the amount of

the precipitate formed increases, the hydrogenating catalytic activity also rises and the position of the maximum on the curve showing the dependence of the catalyst activity on the Al/Co ratio in Fig. 1 shifts to higher values.

ESR spectra of the catalytic systems in hexane or heptane show only broad signal II. The precipitate is formed more rapidly for **2** containing crystallization water. In this case, the formation and aggregation of nanoscale particles proceeds much easier due to the absence of arenes forming mononuclear Co(0) complexes as follows from the absence of signal III in the ESR spectrum. For low $C_{Co} = 2$ mmol/L no precipitate is formed and UV spectra do not show any turbidity of the solutions, suggesting that the process of aggregation is retarded. Extremely high TOF for hydrogenation of 1-hexene at $C_{Co} = 0.25$ mmol/L supports this conclusion.

References

[1] K. Ziegler, H.G. Gelbert, E. Holzkamp, G. Wilke, Ann. Chem. 629 (3) (1960) 172.
[2] M.F. Śloan, A.S. Matlack, D.S. Breslow, J. Am. Chem. Soc. 85 (24) (1963) 4014.
[3] I.V. Kalechitz, F.K. Shmidt, Kinet. Catal. 7 (3) (1966) 614.
[4] R. Stern, L. Sajus, Tetrahedron Lett. 60 (1968) 6313.
[5] I.V. Kalechitz, V.G. Lipovich, F.K. Shmidt, Neftekhimiya 6 (1966) 813.
[6] V.S. Feldblum, N.V. Obeschalova, A.I. Lescheva, Dokl. AN SSSR 172 (1) (1967) 111.
[7] Yu.B. Monakov, I.R. Mullagaliev, Russ. Chem. Bull. 53 (1) (2004) 1.
[8] G. Wilke, Angew. Chem. Int. Ed. 42 (41) (2003) 5000.
[9] L.L. Böhm, Angew. Chem. Int. Ed. 42 (41) (2003) 5010.
[10] G. Natta, Chem. Ind. (1965) 823.
[11] A.L. McKnight, R.M. Waymouth, Chem. Rev. 98 (7) (1998) 2587.
[12] G.L. Tembe, A.R. Bandyopadhyay, S.M. Pillai, S. Satish, M. Ravindranathan, Angew. Makromol. Chem. 225 (1) (1995) 51.
[13] L.A. Nekhaeva, G.N. Bondarenko, V.M. Frolov, Kinet. Catal. 44 (5) (2003) 692.
[14] V.G. Lipovich, F.K. Shmidt, I.V. Kalechitz, Kinet. Catal. 8 (4) (1967) 812.
[15] V.G. Lipovich, F.K. Shmidt, I.V. Kalechitz, Kinet. Catal. 8 (6) (1967) 1099.
[16] W.R. Kroll, J. Catal. 15 (3) (1969) 281.
[17] I.V. Nicolesku, E. Angelesku, J. Pol. Sci.: PA-1 4 (12) (1966) 2963.
[18] K. Tamai, T. Saito, Y. Uchida, A. Misono, Bull. Chem. Soc. 38 (10) (1965) 1575.
[19] V.V. Sarayev, F.K. Shmidt, V.G. Lipovich, S.M. Krasnopol'skaya, Kinet. Catal. 14 (2) (1973) 477.
[20] V.V. Sarayev, F.K. Shmidt, G.M. Larin, V.G. Lipovich, Izv. AN SSSR 11 (1974) 211.
[21] F.K. Shmidt, Kataliz Kompleksami Metallov Pervogo Perekhodnogo Rjada Reaktsii Gidrirovanija I Dimerizatsii, Edition of Irkutsk State University, Irkutsk, 1986, 230 pp.
[22] F.K. Shmidt, V.V. Sarayev, Y.S. Levkovskii, V.G. Lipovich, V.A. Gruznykh, G.V. Ratovskii, T.V. Dmitrieva, L.O. Nindakova, React. Kinet. Catal. Lett. 10 (2) (1979) 195.
[23] G.V. Ratovskii, T.V. Dmitrieva, L.O. Nindakova, F.K. Shmidt, Koord. Khim. 6 (1) (1980) 61.
[24] T.V. Dmitrieva, G.V. Ratovskii, L.O. Nindakova, F.K. Shmidt, React. Kinet. Catal. Lett. 11 (2) (1979) 121.
[25] J. Barrault, M. Blanchard, A. Derouault, M. Ksibi, M.I. Zaki, J. Mol. Catal. A 93 (3) (1994) 289.
[26] S. Pasynkiewicz, A. Pietrzykowki, K. Dowbor, J. Organomet. Chem. 78 (1) (1974) 55.
[27] A. Gordon, R. Ford, A Handbook of Practical Data, Techniques and References, John Wiley & Sons, NY/London/Sydney/Toronto, 1972, 520 pp.
[28] N.N. Korneev, A.F. Popov, B.A. Krentsel, Kompleksnye metallorganicheskie katalizatory, Khimija, Leningrad, 1969, 208 pp.
[29] V.V. Kafarov (Ed.), Spravochnik po rastvorimosti, vol. 1, AN SSSR, Moscow/Leningrad, 1962, 1958 pp.
[30] P.A. Frolovskii, Khromatografija gazov, Nedra, Moscow, 1969, 214 pp.
[31] H. Bönnemann, W. Brijoux, R. Brinkmann, U. Endruschat, W. Hofstadt, K. Angermund, Rev. Roum. Chim. 44 (11–12) (1999) 1003.
[32] J.A. Widegren, R.G. Finke, J. Mol. Catal. A 198 (1–2) (2003) 317.
[33] F.K. Shmidt, V.V. Sarayev, S.M. Krasnopol'skaya, V.G. Lipovich, Kataliticheskie prevraschenija uglevodorodov, Edition of Irkutsk State University, Irkutsk, 1974, 195 pp.
[34] C.L. Kwan, J.K. Kochi, J. Am. Chem. Soc. 98 (16) (1976) 4903.
[35] V.V. Sarayev, F.K. Shmidt, Yu.S. Levkovskii, V.A. Gruznykh, G.M. Larin, N.D. Malakhova, Koord. Khim. 5 (8) (1979) 1190.
[36] V.V. Sarayev, F.K. Shmidt, J. Mol. Catal. A 158 (2) (2000) 149.
[37] V.V. Sarayev, F.K. Shmidt, Elektronnyi paramagnitnyi rezonans metallokompleksnykh katalizatorov, Edition of Irkutsk State University, Irkutsk, 1985, 334 p.
[38] V.V. Sarayev, L.O. Nindakova, O.M. Reshetnikova, S.R. Grefenshtein, Koord. Khimija 13 (2) (1987) 199.
[39] K. Nakomoto, IR Spectra of Inorganic and Coordination Compounds, second ed., Wiley, NY, 1970.
[40] V.V. Skopenko, V.M. Amirkhanov, T.Yu. Sliva, I.S. Vasilchenko, E.L. Anpilova, A.D. Garnovski, Russ. Chem. Rev. 73 (8) (2004) 737.
[41] M.I. Prince, K. Weiss, J. Organomet. Chem. 2 (2) (1964) 166.
[42] M.J. Gibian, R.C. Corley, Chem. Rev. 73 (5) (1973) 441.
[43] K. Fischer, K. Jones, P. Mischbach, P. Stabba, G. Wilke, Angew. Chem. 85 (23) (1973) 1002.
[44] C. Eden, H. Feilchenfeld, Tetrahedron 18 (2) (1962) 233.
[45] A.I. Kitaigorodskii, Rentgenostrukturnyi analiz melkokristallicheskikh I amorfnykh tel, Gos. Izd. Tekh.-Teor. Lit., Moscow/Leningrad, 1952, 588 pp.
[46] H. Lipson, H. Steeple, Interpretation of X-Ray Powder Diffraction Patterns, Markins Press, NY, 1970.
[47] A. Furstner (Ed.), Active Metals: Preparation, Characterization, Application, VCH, Weinheim, 1996, 464 pp.
[48] Yu.I. Petrov, Fizika malykh chastits, Nauka, Moscow, 1982, 380 pp.
[49] P.A. Chernavskii, G.V. Pankina, A.S. Lermontov, V.V. Lunin, Kinet. Catal. 44 (5) (2003) 718.
[50] S.P. Gubin, Russ. Khim. Zhurn. 44 (6) (2000) 23.
[51] H. Bönnemann, W. Brijoux, R. Brinkmann, N. Matoussevitch, N. Waldöfner, N. Palina, H. Modrow, Inorg. Chim. Acta 350 (4) (2003) 617.
[52] H. Bönnemann, N. Waldöfner, H.-G. Haubold, T. Vad, Chem. Mater. 14 (3) (2002) 1115.